**Competing interests**
The authors declare that they have no competing interests.

**Authors' contributions**
HT conceived the study, acquired data of IHC and FISH, analyzed data, and prepared manuscript. MK and SU also conceived the study, acquired data of IHC and analyzed data. SY and TK acquired data of FISH and analyzed data. RYO also conceived the study and supervised the analysis. All authors read and approved the final manuscript.

**Acknowledgements**
This study was supported in part by a grant-in-aid for Cancer Research from the Ministry of Health, Labor, and Welfare, Japan and a grant-in-aid from the Foundation for Promotion of Defense Medicine, Tokorozawa, Japan. We are grateful to Dr. Yutaka Hatanaka, Department of Medical Science, Dako Japan Inc., Kyoto, for immunohistochemistry and to Ms. Kozue Suzuki, Department of Basic Pathology, National Defense Medical College, Tokorozawa, for FISH. We thank Dr. Futoshi Akiyama, Department of Clinical Pathology, Cancer Institute, Tokyo; Dr. Yutaka Tokuda, Department of Surgery, Tokai University School of Medicine, Isehara; Dr. Masakazu Toi, Department of Breast Surgery, Kyoto University Graduate School of Medicine, Kyoto; Dr. Toru Watanabe, Hamamatsu Oncology Center, Hamamatsu; and Dr. Goi Sakamoto, Sakamoto Memorial Clinic Academy of Breast Pathology, Tokyo, for their critical advice.

**Author details**
[1]Diagnostic Pathology Section, Clinical Laboratory Division, National Cancer Center Hospital, 5-1-1 Tsukiji, Chuo-ku, Tokyo 104-0045, Japan. [2]Department of Pathology, Saitama Cancer Center Hospital, 818 Komuro, Ina-machi, Kitaadachi-gun, Saitama 362-0806, Japan. [3]Department of Pathology, Tokai University School of Medicine, Shimokasuya 143, Isehara, Kanagawa 259-1193, Japan. [4]Department of Basic Pathology, National Defense Medical College, 3-2 Namiki, Tokorozawa, Saitama 359-8513, Japan.

**Received: 20 February 2010 Accepted: 7 October 2010**
**Published: 7 October 2010**

**References**

1. Slamon DJ, Clark GM, Wong SG, Levin WJ, Ullrich A, McGuire WL: **Human breast cancer: correlation of relapse and survival with amplification of the *HER-2/neu* oncogene.** *Science* 1987, **235**:177-182.
2. Kallioniemi OP, Kallioniemi A, Kurisu W, Thor A, Chen LC, Smith HS, Waldman FM, Pinkel D, Gray JW: ***ERBB2* amplification in breast cancer analyzed by fluorescence in situ hybridization.** *Proc Natl Acad Sci USA* 1992, **89**:5321-5325.
3. Chia S, Norris B, Speers C, Cheang M, Gilks B, Gown AM, Huntsman D, Olivotto IA, Nielsen TO, Gelmon K: **Human epidermal growth factor receptor 2 overexpression as a prognostic factor in a large tissue microarray series of node-negative breast cancers.** *J Clin Oncol* 2008, **26**:5697-5704.
4. Slamon DJ, Leyland-Jones B, Shak S, Fuchs H, Paton V, Bajamonde A, Fleming T, Eiermann W, Wolter J, Pegram M, Baselga J, Norton L: **Use of chemotherapy plus a monoclonal antibody against HER2 for metastatic breast cancer that overexpresses HER2.** *N Engl J Med* 2001, **344**:783-792.
5. Romond EH, Perez EA, Bryant J, Suman VJ, Geyer CE Jr, Davidson NE, Tan-Chiu E, Martino S, Paik S, Kaufman PA, Swain SM, Pisansky TM, Fehrenbacher L, Kutteh LA, Vogel VG, Visscher DW, Yothers G, Jenkins RB, Brown AM, Dakhil SR, Mamounas EP, Lingle WL, Klein PM, Ingle JN, Wolmark N: **Trastuzumab plus adjuvant chemotherapy for operable HER2-positive breast cancer.** *N Engl J Med* 2005, **353**:1673-1684.
6. Piccart-Gebhart MJ, Procter M, Leyland-Jones B, Goldhirsch A, Untch M, Smith I, Gianni L, Baselga J, Bell R, Jackisch C, Cameron D, Dowsett M, Barrios CH, Steger G, Huang CS, Andersson M, Inbar M, Lichinitser M, Láng I, Nitz U, Iwata H, Thomssen C, Lohrisch C, Suter TM, Rüschoff J, Suto T, Greatorex V, Ward C, Straehle C, McFadden E, Dolci MS, Gelber RD: **Herceptin Adjuvant (HERA) Trial Study Team. Trastuzumab after adjuvant chemotherapy in HER2-positive breast cancer.** *N Engl J Med* 2005, **353**:1659-1672.
7. Joensuu H, Kellokumpu-Lehtinen PL, Bono P, Alanko T, Kataja V, Asola R, Utriainen T, Kokko R, Hemminki A, Tarkkanen M, Turpeenniemi-Hujanen T, Jyrkkiö S, Flander M, Helle L, Ingalsuo S, Johansson K, Jääskeläinen AS, Pajunen M, Rauhala M, Kaleva-Kerola J, Salminen T, Leinonen M, Elomaa I, Isola J, FinHer Study Investigators: **Adjuvant docetaxel or vinorelbine with or without trastuzumab for breast cancer.** *N Engl J Med* 2006, **354**:809-820.
8. Buzdar AU, Valero V, Ibrahim NK, Francis D, Broglio KR, Theriault RL, Pusztai L, Green MC, Singletary SE, Hunt KK, Sahin AA, Esteva F, Symmans WF, Ewer MS, Buchholz TA, Hortobagyi GN: **Neoadjuvant therapy with paclitaxel followed by 5-fluorouracil, epirubicin, and cyclophosphamide chemotherapy and concurrent trastuzumab in human epidermal growth factor receptor 2-positive operable breast cancer: an update of the initial randomized study population and data of additional patients treated with the same regimen.** *Clin Cancer Res* 2007, **13**:228-233.
9. Hurley J, Doliny P, Reis I, Silva O, Gomez-Fernandez C, Velez P, Pauletti G, Powell JE, Pegram MD, Slamon DJ: **Docetaxel, cisplatin, and trastuzumab as primary systemic therapy for human epidermal growth factor receptor 2-positive locally advanced breast cancer.** *J Clin Oncol* 2006, **24**:1831-1838.
10. Wolff AC, Hammond ME, Schwartz JN, Hagerty KL, Allred DC, Cote RJ, Dowsett M, Fitzgibbons PL, Hanna WM, Langer A, McShane LM, Paik S, Pegram MD, Perez EA, Press MF, Rhodes A, Sturgeon C, Taube SE, Tubbs R, Vance GH, van de Vijver M, Wheeler TM, Hayes DF: **American Society of Clinical Oncology/College of American Pathologists guideline recommendations for human epidermal growth factor receptor 2 testing in breast cancer.** *J Clin Oncol* 2007, **25**:118-145.
11. Carlson RW, Moench SJ, Hammond ME, Perez EA, Burstein HJ, Allred DC, Vogel CL, Goldstein LJ, Somlo G, Gradishar WJ, Hudis CA, Jahanzeb M, Stark A, Wolff AC, Press MF, Winer EP, Paik S, Ljung BM: **NCCN HER2 Testing in Breast Cancer Task Force. HER2 testing in breast cancer: NCCN Task Force report and recommendations.** *J Natl Compr Canc Netw* 2006, **4(Suppl 3)**:S1-S22.
12. Sauter G, Lee J, Bartlett JM, Slamon DJ, Press MF: **Guidelines for human epidermal growth factor receptor 2 testing: biologic and methodologic considerations.** *J Clin Oncol* 2009, **27**:1323-1333.
13. Tsuda H, Akiyama F, Terasaki H, Hasegawa T, Kurosumi M, Shimadzu M, Yamamori S, Sakamoto G, Detection of HER-2/neu (c-erbB-2) DNA amplification in primary breast carcinoma: **Interobserver reproducibility and correlation with immunohistochemical HER-2 overexpression.** *Cancer* 2001, **92**:2965-2974.
14. Press MF, Sauter G, Bernstein L, Villalobos IE, Mirlacher M, Zhou JY, Wardeh R, Li YT, Guzman R, Ma Y, Sullivan-Halley J, Santiago A, Park JM, Riva A, Slamon DJ: **Diagnostic evaluation of HER-2 as a molecular target: an assessment of accuracy and reproducibility of laboratory testing in large, prospective, randomized clinical trials.** *Clin Cancer Res* 2005, 11:6598-6607.
15. Tsuda H, Sasano H, Akiyama F, Kurosumi M, Hasegawa T, Osamura RY, Sakamoto G: **Evaluation of interobserver agreement in scoring immunohistochemical results of HER-2/neu (c-erbB-2) expression detected by HercepTest, Nichirei polyclonal antibody, CB11 and TAB250 in breast carcinoma.** *Pathol Int* 2002, **52**:126-134.
16. Umemura S, Osamura RY, Akiyama F, Honma K, Kurosumi M, Sasano H, Toyoshima S, Tsuda H, Rüschoff J, Sakamoto G: **What causes discrepancies in HER2 testing for breast cancer? A Japanese ring study in conjunction with the global standard.** *Am J Clin Pathol* 2008, **130**:883-891.
17. Roche PC, Suman VJ, Jenkins RB, Davidson NE, Martino S, Kaufman PA, Addo FK, Murphy B, Ingle JN, Perez EA: **Concordance between local and central laboratory HER2 testing in the breast intergroup trial N9831.** *J Natl Cancer Inst* 2002, **94**:855-857.
18. Paik S, Bryant J, Tan-Chiu E, Romond E, Hiller W, Park K, Brown A, Yothers G, Anderson S, Smith R, Wickerham DL, Wolmark N: **Real-world performance of HER2 testing–National Surgical Adjuvant Breast and Bowel Project experience.** *J Natl Cancer Inst* 2002, **94**:852-854.
19. Reddy JC, Reimann JD, Anderson SM, Klein PM: **Concordance between central and local laboratory HER2 testing from a community-based clinical study.** *Clin Breast Cancer* 2006, **7**:153-157.
20. Bast RC Jr, Ravdin P, Hayes DF, Bates S, Fritsche H Jr, Jessup JM, Kemeny N, Locker GY, Mennel RG, Somerfield MR: **American Society of Clinical Oncology Tumor Markers Expert Panel. 2000 update of recommendations for the use of tumor markers in breast and colorectal cancer: clinical practice guidelines of the American Society of Clinical Oncology.** *J Clin Oncol* 2001, **19**:1865-1878.

21. Usami S, Moriya T, Amari M, Suzuki A, Ishida T, Sasano H, Ohuchi N: **Reliability of prognostic factors in breast carcinoma determined by core needle biopsy.** *Jpn J Clin Oncol* 2007, **37**:250-255.
22. Apple SK, Lowe AC, Rao PN, Shintaku IP, Moatamed NA: **Comparison of fluorescent in situ hybridization HER2/neu results on core needle biopsy and excisional biopsy in primary breast cancer.** *Mod Pathol* 2009, **22**:1151-1159.
23. Arnedos M, Nerurkar A, Osin P, A'hern R, Smith IE, Dowsett M: **Discordance between core needle biopsy (CNB) and excisional biopsy (EB) for estrogen receptor (ER), progesterone receptor (PgR) and HER2 status in early breast cancer (EBC).** *Ann Oncol* 2009, **20**:1948-1952.
24. Brunelli M, Manfrin E, Martignoni G, Miller K, Remo A, Reghellin D, Bersani S, Gobbo S, Eccher A, Chilosi M, Bonetti F: **Genotypic intratumoral heterogeneity in breast carcinoma with HER2/neu amplification: evaluation according to ASCO/CAP criteria.** *Am J Clin Pathol* 2009, **131**:678-682.
25. Chivukula M, Bhargava R, Brufsky A, Surti U, Dabbs DJ: **Clinical importance of HER2 immunohistologic heterogeneous expression in core-needle biopsies vs resection specimens for equivocal (immunohistochemical score 2+) cases.** *Mod Pathol* 2008, **21**:363-368.
26. Fleiss JL: **Measuring nominal scale agreement among many raters.** *Psychol Bull* 1971, **76**:378-382.
27. Landis JR, Koch GG: **The measurement of observer agreement for catetgorical data.** *Biometrics* 1977, **33**:159-174.
28. D'Alfonso T, Liu YF, Monni S, Rosen PP, Shin SJ: **Accurately assessing her-2/neu status in needle core biopsies of breast cancer patients in the era of neoadjuvant therapy: emerging questions and considerations addressed.** *Am J Surg Pathol* 2010, **34**:575-581.
29. Moelans CB, de Weger RA, van Blokland MT, Ezendam C, Elshof S, Tilanus MG, van Diest PJ: **HER-2/neu amplification testing in breast cancer by multiplex ligation-dependent probe amplification in comparison with immunohistochemistry and in situ hybridization.** *Cell Oncol* 2009, **31**:1-10.
30. Shousha S, Peston D, Amo-Takyi B, Morgan M, Jasani B: **Evaluation of automated silver-enhanced in situ hybridization (SISH) for detection of HER2 gene amplification in breast carcinoma excision and core biopsy specimens.** *Histopathology* 2009, **54**:248-253.
31. Wolf V, Große R, Erggelet J, Holzhausen HJ, Hauptmann S, Thomssen C: **The reliability of HER2-status determination from core-needle-biopsies and surgical specimens: A comparison of two established test methods (IHC, CISH).** *J Clin Oncol* 2009, **27**:15S, (suppl. Abstr. e22141).
32. Gruver AM, Peerwani Z, Tubbs RR: **Out of the darkness and into the light: bright field in situ hybridisation for delineation of ERBB2 (HER2) status in breast carcinoma.** *J Clin Pathol* 2010, **63**:210-219.
33. Hiroi S, Tsuda H, Oya T, Hayama T, Kawai T, Torikata C: **Influence of fixation period on the detection of HER2/neu protein and *HER2/neu* gene signals.** *Proc Jpn Soc Pathol* 2003, **92**:222, (abstract in Japanese).
34. Terry J, Torlakovic EE, Garratt J, Miller D, Köbel M, Cooper J, Bahzad S, Pilavdzic D, O'Malley F, O'Brien AE, SenGupta S, Alport E, Têtu B, Knight B, Pettigrew NM, Berendt R, Wolber R, Trotter MJ, Riddell RH, Gaboury L, Elms F, Magliocco A, Barnes P, Gown AM, Gilks CB: **Implementation of a Canadian external quality assurance program for breast cancer biomarkers: an initiative of Canadian Quality Control in immunohistochemistry (cIQc) and Canadian Association of Pathologists (CAP) National Standards Committee/Immunohistochemistry.** *Appl Immunohistochem Mol Morphol* 2009, **17**:375-382.
35. Dowsett M, Hanby AM, Laing R, Walker R, National HER2 Consultation Steering Group: **HER2 testing in the UK: consensus from a national consultation.** *J Clin Pathol* 2007, **60**:685-689.

**Pre-publication history**
The pre-publication history for this paper can be accessed here:
http://www.biomedcentral.com/1471-2407/10/534/prepub

doi:10.1186/1471-2407-10-534
**Cite this article as:** Tsuda *et al.*: HER2 testing on core needle biopsy specimens from primary breast cancers: interobserver reproducibility and concordance with surgically resected specimens. *BMC Cancer* 2010 **10**:534.

The Breast Journal

LETTER TO THE EDITOR

# Early Reduction in Standardized Uptake Value After One Cycle of Neoadjuvant Chemotherapy Measured by Sequential FDG PET/CT is an Independent Predictor of Pathological Response of Primary Breast Cancer

To the Editor:

$^{18}$F-fluorodeoxyglucose (FDG) levels on positron emission tomography (PET) reflect glucose metabolism in cancer cells (1). Currently, FDG PET combined with computed tomography (FDG PET/CT) has become employed as a non-invasive method for imaging glucose metabolism in tumors (2,3). The aim of the present study was to evaluate whether early metabolic changes after one cycle of neoadjuvant chemotherapy in FDG uptake evaluated by maximal standardized uptake value ($SUV_{max}$) could predict a pathological response of primary breast cancers.

Thirty-two tumors in 30 patients having primary invasive breast cancer were investigated. All patients had received a standard neoadjuvant chemotherapy regimen comprising four cycles of epirubicine (90 mg/m$^2$) and cyclophosphamide (600 mg/m$^2$) on a triweekly basis and sequential use of 12 cycles of weekly paclitaxel (80 mg/m$^2$) (25 patients) or four cycles of triweekly docetaxel (60 mg/m$^2$) (five patients). The procedure of FDG PET/CT has been described (4). Sequential FDG PET/CT (Biograph LSO Emotion; 3D model, Siemens, Germany) was performed at the baseline (baseline PET/CT), after one cycle of chemotherapy (PET/CT2), after four cycles of chemotherapy (PET/CT3), and prior to surgery (PET/CT4). Tumors showing a 40% reduction or more in $SUV_{max}$ on PET/CT2, when compared with the baseline PET/CT, were defined as metabolic responders and those showing a change of less than 40% in $SUV_{max}$ were considered to be metabolic nonresponders (Fig. 1).

Address corresopondence and reprint requests to: Hitoshi Tsuda, MD, PhD, Department of Basic Pathology, National Defense Medical College, 3-2 Namiki, Tokorozawa, Saitama 359-8513, Japan, or e-mail: hstsuda@gmail.com.

DOI: 10.1111/j.1524-4741.2010.01011.x

 1075-122X/10
The Breast Journal, Volume 16 Number 6, 2010 660–662

Baseline characteristics of patients and tumors, determined by conventional modalities, are shown in Table 1. Baseline $SUV_{max}$ was significantly higher in metabolic responders [10.2 ± 6.4 SD] than nonresponders (6.7 ± 3.1 SD) ($p = 0.05$). The percentage of tumors with nuclear grade 3 was significantly higher among the metabolic responders (71%) than among the nonresponders (16%) ($p = 0.03$). There were no significant differences between metabolic responders and nonresponders with regard to patient age, T-stage, nodal status, hormone receptor status, or HER2 status.

The average degree of decrease in $SUV_{max}$ at PET/CT2 in comparison with the baseline $SUV_{max}$ was 57.9% (±11.7 SD) in metabolic responders and 10.3% (±15.7 SD) in metabolic nonresponders ($p < 0.0001$). Clinical response after completion of chemotherapy was measured using ultrasound or CT combined with FDG PET, and evaluated based on RECIST. On the basis of clinical response, five (71%) and two (29%) of the seven tumors with a metabolic response exhibited partial response (PR) and complete response (CR), respectively, while 18 (72%) of the 25 nonresponding tumors had PR. No nonresponding tumors showed CR. Metabolic responders showed a significantly excellent clinical response rate (100%) in terms of PR or CR in comparison with that (72%) for non-responding tumors ($p = 0.001$) (Table 2a).

Histological criteria for assessment of therapeutic response were based on General Rules for Clinical and Pathological Recording of Breast Cancer 2008 (5). Among a total of 32 tumors, six (19%) and two (6%) were found to have grade 3, or pathological complete response (pCR), and to have grade 2b, or near pCR, where only a few residual invasive cancer cells were seen, respectively. Among the seven tumors with a metabolic response, three (43%) and two (29%) showed pCR and near pCR, respectively. Among the 25 tumors without metabolic response,

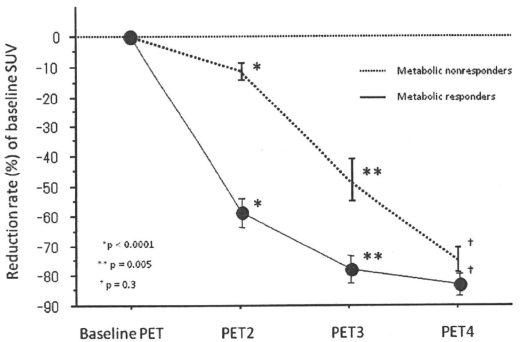


**Figure 1.** Reduction in standarized uptake value (SUV) of primary breast cancer after adjuvant chemotherapy, detected by FDG PET/CT. Mean reduction rate of SUV during neoadjuvant chemotherapy was significantly different at PET/CT2 ($p < 0.0001$) and at PET/CT3 ($p = 0.005$) but not at PET/CT4 ($p = 0.3$) between tumors showing,and not showing a metabolic response. Thirty-two tumors were divided into metabolic responders and metabolic nonresponders based on a cut-off value of 40% reduction in SUV at PET/CT2 compared with baseline PET/CT.

**Table 1. Patients and tumors characteristics between metabolic responders and nonresponders**

| Variables | Total $n = 32$ (%) | Responder $n = 7$ (%) | Nonresponder $n = 25$ (%) | p-value |
|---|---|---|---|---|
| Age, years (average ± SD) | 54.9 ± 10.1 | 58.9 ± 14.5 | 53.5 ± 8.0 | 0.2 |
| Baseline SUV (average ± SD) | 7.5 ± 4.2 | 10.2 ± 6.4 | 6.7 ± 3.1 | 0.05 |
| T-stage | | | | |
| 1 | 5 (16) | 1 (14) | 4 (16) | 0.3 |
| 2 | 21 (66) | 5 (72) | 16 (64) | |
| 3 | 3 (9) | 0 (0) | 3 (12) | |
| 4 | 3 (9) | 1 (14) | 2 (8) | |
| Nodal status | | | | |
| Negative | 14 (4) | 3 (43) | 11 (44) | 0.9 |
| Positive | 18 (5) | 4 (57) | 14 (56) | |
| Nuclear grade | | | | |
| 1 and 2 | 23 (72) | 2 (29) | 22 (88) | 0.03 |
| 3 | 9 (28) | 5 (71) | 3 (12) | |
| Hormone receptor status | | | | |
| ER and/or PR positive | 25 (78) | 4 (57) | 21 (84) | 0.5 |
| ER and PR negative | 7 (22) | 3 (43) | 4 (16) | |
| HER2 status | | | | |
| 0, 1+, 2+ | 25 (78) | 3 (43) | 22 (88) | 0.06 |
| 3+ | 7 (22) | 4 (57) | 3 (12) | |

SD, standard derivation; SUV, standardized uptake value; ER, estrogen receptor; PR, progesterone receptor.

three (12%) showed pCR, but none showed near pCR. Tumors showing a metabolic response showed a significantly higher percentage of pCR/near pCR than tumors showing no metabolic response ($p = 0.01$) (Table 2b).

**Table 2. Clinical and pathological response to neoadjuvant chemotherapy between metabolic responders and nonresponders**

(a) Post-chemotherapeutic clinical response

| | PD | SD | PR | CR | Total |
|---|---|---|---|---|---|
| Metabolic responder | 0 | 0 | 5 | 2 | 7 |
| Metabolic nonresponder | 2 | 5 | 18 | 0 | 25 |
| Total | 2 | 5 | 23 | 2 | 32 |
| | | | | | $p = 0.001$ |

(b) Post-chemotherapeutic pathological response

| | pPD | pPR | Near pCR | pCR | Total |
|---|---|---|---|---|---|
| Metabolic responder | 0 | 2 | 2 | 3 | 7 |
| Metabolic nonresponder | 1 | 21 | 0 | 3 | 25 |
| Total | 1 | 23 | 2 | 6 | 32 |
| | | | | | $p = 0.01$ |

PD, progressive disease; SD, stable disease; PR, partial response; CR, complete response; pCR, pathological CR.

Univariate analysis showed that metabolic response [$p = 0.005$, hazard ratio (HR) = 18.3, 95% confidential interval (CI) 2.4–140.4], HER2 overexpression ($p = 0.005$, HR = 18.3, 95% CI 2.4–140.4), and hormone-receptor negativity ($p = 0.04$, HR = 7.0, 95% CI 1.1–44.1) were predictive of pCR/near-pCR to neoadjuvant chemotherapy. Nuclear grade was

marginally associated with pCR/near-pCR (p = 0.1, HR = 4.2, 95% CI 0.6–27.4). No significant association between other factors and pCR/near-pCR was found. Multivariate analysis employing a logistic regression model showed that metabolic response remained an independent variable for predicting pCR/near-pCR (p = 0.05, HR = 11.9, 95% CI 1.1–104.9), but HER2 overexpression and hormone-receptor negativity were not (p = 0.1 and 0.4 respectively).

This study indicated that assessment of FDG PET/CT after one cycle of chemotherapy has independent value for early prediction of a pathologic response of primary breast cancer to standard neoadjuvant chemotherapy regimen followed by taxane.

**Acknowledgments**

This work was supported by the grants for the promotion of Defense Medicine from the Ministry of Defense, Japan and Department of Breast Oncology on International Medical Center in Saitama Medical University.

Shigeto Ueda, MD[*]
Hitoshi Tsuda, MD, PhD[¶]
Toshiaki Saeki, MD, PhD[†,‡]
Akihiko Osaki, MD, PhD[†,‡]
Takashi Shigekawa, MD[†,‡]
Jiro Ishida, MD, PhD[§]
Katsumi Tamura, MD[§]
Yoshiyuki Abe, MD, PhD[§]
Jiro Omata, MD[*]
Tomoyuki Moriya, MD, PhD[*]
Kazuhiko Fukatsu, MD, PhD[*]
Junji Yamamoto, MD, PhD[*]

[*]Department of Surgery, National Defense Medical College, Tokorozawa, Saitama, Japan; [†]Department of Breast Oncology, Tokorozawa Ichou Hospital, Tokorozawa, Saitama, Japan; [‡]Department of Breast Oncology, Saitama Medical University, International Medical Center, Saitama, Japan; [§]Tokorozawa PET Diagnostic Imaging Clinic, Tokorozawa, Saitama, Japan; and [¶]Department of Basic Pathology, National Defense Medical College, Tokorozawa, Saitama, Japan

## REFERENCES

1. Juweid ME, Cheson BD. Positron-emission tomography and assessment of cancer therapy. *N Engl J Med* 2006;354:496–507.

2. Schelling M, Avril N, Nahrig J, *et al.* Positron emission tomography using [(18)F]Fluorodeoxyglucose for monitoring primary chemotherapy in breast cancer. *J Clin Oncol* 2000;18:1689–95.

3. Rousseau C, Devillers A, Sagan C, *et al.* Monitoring of early response to neoadjuvant chemotherapy in stage II and III breast cancer by [18F] fluorodeoxyglucose positron emission tomography. *J Clin Oncol* 2006;24:5366–72.

4. Ueda S, Tsuda H, Asakawa H, *et al.* Clinicopathological and prognostic relevance of uptake level using 18F-fluorodeoxyglucose positron emission tomography/computed tomography fusion imaging (18F-FDG PET/CT) in primary breast cancer. *Jpn J Clin Oncol* 2008;38:250–8.

5. Sakamoto G, Inaji H, Akiyama F, *et al.* General rules for clinical and pathological recording of breast cancer 2008. *Breast Cancer* 2008;12(Suppl):S1–27.

Breast Cancer (2011) 18:18–23
DOI 10.1007/s12282-010-0215-8



# Histopathological effect of radiofrequency ablation therapy for primary breast cancer, with special reference to changes in cancer cells and stromal structure and a comparison with enzyme histochemistry

**Kunihiko Seki · Hitoshi Tsuda · Eriko Iwamoto · Takayuki Kinoshita**

Received: 7 April 2010 / Accepted: 7 June 2010 / Published online: 4 August 2010


**Abstract** Radiofrequency ablation (RFA) therapy is expected to be applicable to small breast cancers, but no criteria for its histopathological effect have yet been established. Using samples obtained from 15 patients who had undergone RFA and subsequent mastectomy, we compared the histopathological changes in the ablated area with the results of histochemical staining based on the reduction of nitroblue tetrazolium chloride (NBT) by nicotinamide adenine dinucleotide (NADH) diaphorase in frozen tissue sections, and looked for histological changes indicative of the effect of RFA on breast cancer. Grossly, the ablated area in most of the tumors was rough, gritty, less moist, and surrounded by a red congestive limbic zone. The ablated area showed no staining by the NADH diaphorase reaction, and cancer cells in the area showed marked destruction characterized by an unclear intercellular boundary, elongated eosinophilic cytoplasm, pyknotic "streaming" nuclei, and a poorly defined nuclear and cytoplasmic texture. At the same time, fibrous connective tissue also showed degenerative changes, becoming densely homogeneous with loss of its delicate wavy structure. The area in which RFA appeared to have been histopathologically effective was mostly concordant with the area in which the NADH diaphorase reaction was negative. In the periphery of the ablated area, however, cellular changes caused by RFA were less marked, although the NADH diaphorase reaction was visualized with NBT. A larger number of cases should be examined in order to establish criteria for the histopathological effect of RFA on breast cancer.

**Keywords** Breast cancer · Radiofrequency ablation therapy · NADH diaphorase reaction · Histopathological criteria for therapeutic effect

K. Seki (✉)
Clinical Laboratory Division, JR Tokyo General Hospital, 2-1-3 Yoyogi, Shibuya-ku, Tokyo 151-8528, Japan
e-mail: kunihiko-seki@jreast.co.jp

K. Seki · H. Tsuda
Diagnostic Pathology Division, National Cancer Center Hospital, Tokyo, Japan

E. Iwamoto
Diagnostic Radiology Division, National Cancer Center Hospital, Tokyo, Japan

T. Kinoshita
Breast Surgery Division, National Cancer Center Hospital, Tokyo, Japan

## Introduction

Radiofrequency ablation (RFA) therapy is expected to be applicable to small breast cancers as an effective and safe curative treatment of choice. However, no criteria for defining its therapeutic effect have yet been established. The majority of previous studies have employed histopathological examination of hematoxylin–eosin (HE)-stained sections and the histochemical technique for visualizing the reduction of nitroblue tetrazolium chloride (NBT) by nicotinamide adenine dinucleotide (NADH) diaphorase in frozen sections.

The NAD+/NADH redox reaction is one of the most important in living biologic systems. NADH diaphorase activity judged from the reduction of NBT to formazan via oxidation of NADH is a reliable marker of cell viability. Assay of NADH diaphorase is performed histochemically using fresh frozen tissue sections. When reduced NADH is

oxidized by NADH diaphorase, free electrons are transferred to NBT, which becomes reduced and converted to the blue, water-insoluble dye formazan (Fig. 1). NADH diaphorase becomes bound to the structural components of the cell, thereby permitting histochemical visualization of its intracellular location by the use of NBT. Only viable cells have active diaphorase, whereas this activity seems to subside immediately after cell death.

On the other hand, several previous reports have described criteria for evaluation of the RFA effect. Jeffrey et al. [1] considered the presence of pyknotic nuclei and increased intensity of eosinophilic staining to be characteristics of tissue cautery due to heating. Earashi et al. [2] applied histopathological criteria for assessment of therapeutic response described in the "General Rules for Clinical and Pathological Recording of Breast Cancer". However, no histopathological criteria for the therapeutic effect of RFA have yet been established.

In the present study, on the basis of a comparison of histopathological changes in the ablated area with the results of histochemical assay with NADH diaphorase, we attempted to characterize the histological changes in breast cancer induced by RFA.

## Patients and methods

### RFA study protocol

Patient selection and the RFA protocol have been described previously [3]. Histochemical and histopathological examinations were performed on specimens from 15 patients who had undergone RFA for primary breast cancer and subsequent mastectomy between June 2006 and May 2007.

### Pathological analysis

After ablation, the surgically resected specimen was cut at the maximum diameter of the ablated breast tumor (Fig. 2). Both the ablated and non-ablated areas of each tumor and adjacent tissue were grossly evaluated, focusing particularly on the features of coagulation, congestion, and elasticity. Slices of tissue, each including apparently ablated and non-ablated areas, were obtained and mounted in optimal cutting temperature (OCT) compound. The tissue was then immediately frozen in liquid nitrogen, and cut into sections 8- to 10-μm thick. One of these sections was immediately stained with HE, and the others were stored at −80°C until NADH diaphorase-NBT studies. The remaining surgically resected specimens were fixed in 10% formalin and processed for routine histopathological examination.

### Enzyme histochemical analysis

For enzyme histopathological analysis of ablated breast tumors, frozen tissue sections were incubated for 1 h at 37°C in a solution consisting of 0.8 mg/mL reduced β-NADH (Sigma), 0.5 mg/mL nitroblue tetrazolium (Sigma), and 0.05 M Tris-buffered saline (pH 7.4) (Fig. 3). Each slide was fixed in 10% formalin for 30 min and washed in distilled water for 2 min, then glass coverslips were applied with an aqueous medium.

### Mapping and evaluation

Ablated cells were confirmed to be non-viable by their negativity for the oxidation–reduction reaction mediated by NADH diaphorase, whereas residual viable cells were stained blue. By referring to serial sections stained with

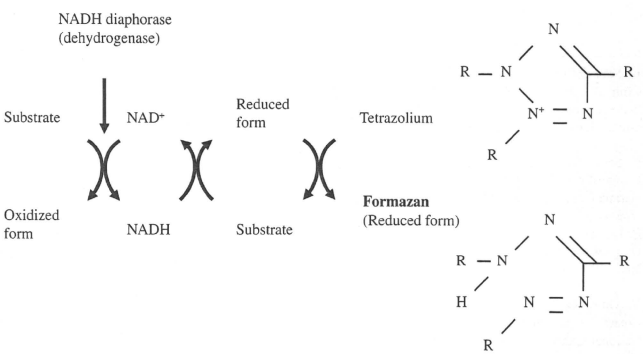


**Fig. 1** Nicotinamide adenine dinucleotide (NADH) redox circuit

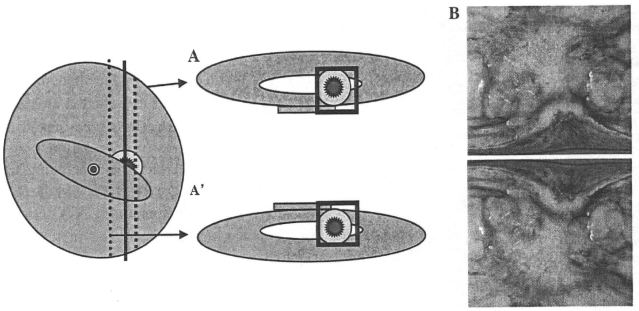


**Fig. 2** Schematic representation of tissue specimens used for evaluation of the histopathological effect of radiofrequency ablation (RFA) to primary breast cancer. **a** An ablated tumor cut at the maximum diameter. The tumor in cut section **a** is taken for NADH diaphorase staining. The tumor in cut section **a'**, the mirror image of section **a**, is taken for routine formalin-fixed and paraffin-embedded blocks. **b** Gross features of the ablated tumor. A congestive limbic zone encircles the ablated area containing the tumor

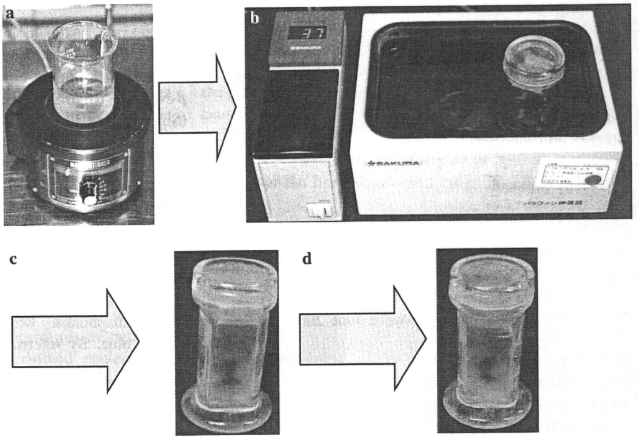


**Fig. 3** Preparation of reagents for histochemical assay of nicotinamide adenine dinucleotide (NADH) diaphorase activity. **a** Adjustment of NADH medium. The incubation medium consists of 0.8 mg/mL reduced $\beta$-NADH (Sigma), 0.5 mg/mL nitroblue tetrazolium, and 0.05 M Tris-buffered saline (pH 7.4), mixed at 37°C. **b** Fresh frozen tissue sections are incubated in the NADH medium in a water bath at 37°C for 1 h. **c** The tissue sections are washed in distilled water for 2 min. **d** These sections are subsequently fixed in 10% formalin for 30 min

both the NADH diaphorase reaction and HE, we compared the histopathological features of stained and adjacent non-stained areas. Gross and histological features attributable to the thermal effects of RFA were investigated by two pathologists (K.S. and H.T.).

## Results

### Gross examination

At the cut surface including the tumor, the ablated area felt firmer and more fragile than the surrounding non-ablated area. The cut surface of the ablated area composed of tumor and fibrous stroma was rough, gritty, and less moist, forming a round, flat surface surrounded by swollen fresh, unablated mammary, and fibroadipose tissue (Fig. 4a). In the central zone of the ablated area, the tumor and fibrous connective tissue were grayish-white to tan in color, forming a fissure or small cavity around the needle track (Fig. 4a). Coagulated non-tumor fibroadipose tissue was also firm and had changed to a tan-yellowish color. A red congestive limbic zone surrounded the ablated area (indicated with dots in Fig. 4a). These congestive rings were observed in 14 of 15 cases.

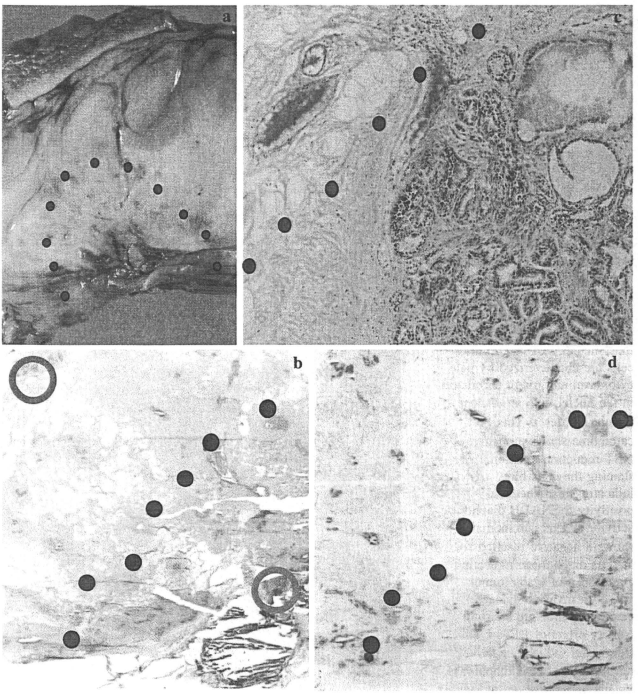


**Fig. 4** Macro- and microscopic features of RFA-treated breast cancer and non-cancerous tissue. **a** Gross features of a mastectomized specimen resected immediately after the RFA procedure. The border between the ablated and non-ablated areas is delineated by a congestive limbic zone (indicated by *dots*). **b** The boundary between the ablated area (*right lower* to *dots*) and non-ablated area (*left upper* to *dots*). A low-magnification view of an HE-stained section. The control part of the ablated area (*red circle*) shows highly degenerative changes. **c** A higher-magnification view of the boundary between the ablated (*right lower* to *dots*) and non-ablated (*left upper* to *dots*) areas. In the latter, congestive blood vessels are evident. In the former, mammary tissue and stroma with mild to moderate heating effects are observed (HE). **d** The boundary between the ablated and non-ablated areas in the serial section of image **b**. The section was subjected to the NADH diaphorase reaction to color viable cells blue due to the reduction of NBT. Only the non-ablated area (*left upper* to *dots*) is stained blue

## Microscopy examination

The boundary between the ablated and non-ablated area was identifiable histologically, although the effect of cautery showed a gradation from strong in the center to mild or moderate at the periphery (Fig. 4b, c). RFA damage to the epithelial cells and fibrous stroma in the ablated area was histologically visualized as follows in HE-stained sections. Epithelial cells, both cancerous and non-cancerous, were characterized by elongated eosinophilic cytoplasm with pyknotic "streaming" nuclei (Fig. 5b). The intercellular boundary and details of the nuclear and cytoplasmic texture were unclear. Fibrous connective tissue also showed degenerative changes resulting in dense homogeneous and highly eosinophilic features (Fig. 6). The original delicate, wavy structure had entirely disappeared. Fibroblasts in the area also showed thermal degenerative changes identical to those seen in epithelial cells.

At the periphery of the ablated area, epithelial cells showed coarse and plain nuclear chromatin due to the thermal effect (Fig. 5c). The boundary between ablated and non-ablated areas was usually characterized by congestive blood vessels, which were grossly evident as a red limbic zone (Fig. 4a). The effects of heating were sometimes relatively mild to moderate near the limbic zone, because the nuclear and cytoplasmic features characteristic of cell death at the periphery of the ablated area adjacent to the red zone were less marked (Fig. 5c) than those in the central ablated area.

## Comparison between NADH diaphorase reaction and histopathological findings

Nicotinamide adenine dinucleotide diaphorase-stained sections showed no reaction in tumor cells at the center of the ablated area, where tumor cells and stroma showed marked heat degeneration. The border between the NADH diaphorase-positive and -negative areas was relatively clear and sharp (Fig. 4d). NADH-positive cells showed the fine structures of intact nuclear chromatin and cytoplasm

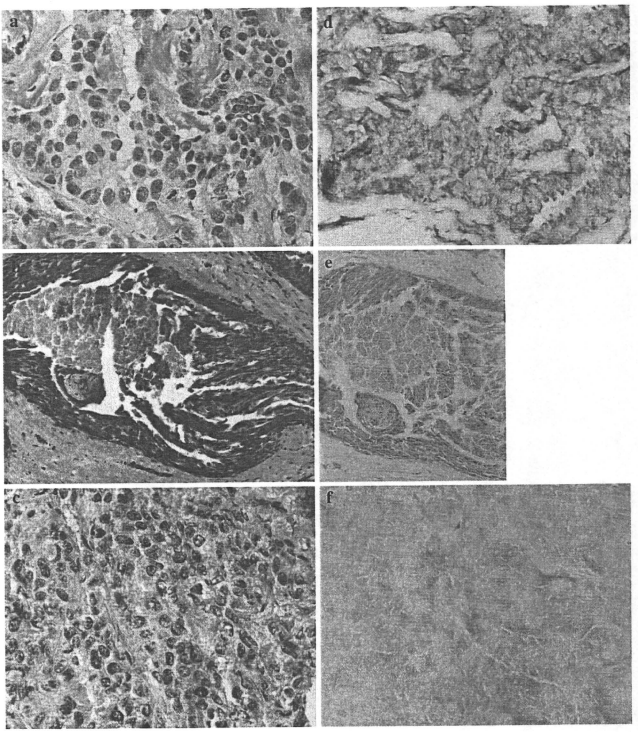


**Fig. 5** Comparison of histopathological features of RFA-treated breast cancer tissue with histochemical results of NADH diaphorase staining. **a**, **d** A non-ablated invasive ductal carcinoma (control specimen). **b**, **e** An invasive ductal carcinoma showing a strong effect of RFA cautery. **c**, **f** An invasive ductal carcinoma showing a moderate heating effect of RFA. **a** Fine structure of the nuclei and cytoplasm of tumor cells, and the collagen fibers of the stoma, are preserved. **b** Ablated tumor cells show an elongated cytoplasm with "streaming-like" nuclei. **c** Ablated tumor cells are characterized by pale cytoplasm and rough chromatin in the nuclei with an unclear cellular border. **d** This carcinoma shows a positive NBT reduction reaction, staining the cells blue, indicating histochemical positivity for NADH diaphorase activity. **e** This carcinoma shows a negative reaction for NADH diaphorase, indicating an absence of viable tumor cells. An invasive ductal carcinoma showing a strong cautery effect of RFA. **f** This carcinoma shows a negative reaction for NADH diaphorase, indicating an absence of viable tumor cells

(Fig. 5a, b), surrounded by a fine, delicate fibrous stroma. In each tumor, the NADH-negative area was approximately equivalent to the area circumscribed by the congestive limbic zone. Neither the central area showing strong effects of cautery, nor the peripheral part of the ablated area showing less marked effects showed the NADH diaphorase reaction (Fig. 5d, f).

## Discussion

We have described the macro- and microscopic findings characteristic of the cautery or heating effect of RFA, based on examination of specimens resected immediately after the procedure. The histopathological features of cellular damage described by some authors have included an unclear intercellular boundary, elongated eosinophilic cytoplasm, pyknotic "streaming" nuclei, and poorly defined nuclear and cytoplasmic texture [1, 4]. In addition, we found that the RFA procedure caused fibrous connective tissue to lose its delicate wavy structure and to degenerate to dense eosinophilic tissue with a loss of fine structure.

The area in which RFA was histologically effective was mostly concordant with the area of NADH diaphorase negativity, especially in the central part of the ablated area. At the periphery, however, cellular change caused by RFA was less marked, and the NADH diaphorase reaction visualized by NBT was usually negative. Fornage et al. described the histopathological changes observed in RFA-treated breast tissues in a study of 21 patients. The changes were similar to those observed in the present study, and were concordant with the results of NADH diaphorase staining [4]. However, a large number of cases should be studied in order to establish criteria for the histopathological effect of RFA. Although the histochemical assay for NADH diaphorase activity is reliable, it cannot always be performed in routine practice. It will therefore be necessary

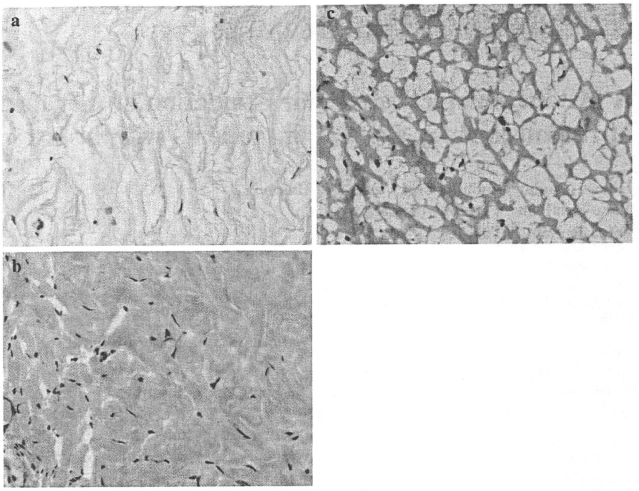


**Fig. 6** **a** Non-ablated stromal tissue in the breast demonstrates the fine wavy structure of collagen fibers (control specimen). **b**, **c** A highly ablated stroma showing eosinophilic and amorphous features without a fine wavy texture. Nuclei of fibroblasts are also pyknotic

to standardize criteria for the effects of RFA that are applicable to formalin-fixed and paraffin-embedded tissue sections.

**Acknowledgments** This work was supported in part by a grant-in-aid for scientific research from the Ministry of Heath, Labor and Welfare, Japan.

## References

1. Jeffrey SS, Birdwell RL, Ikeda DM. Radiofrequency ablation of breast cancer: first report of an emerging technology. Arch Surg. 1999;134:1064–8.
2. Earashi M, Noguchi M, Motoyoshi A, Fujii H. Radiofrequency ablation therapy for small breast cancer followed by immediate surgical resection or delayed mammotome excision. Breast Cancer. 2007;14:39–47.
3. Kinoshita T, Iwamoto E, Tsuda H, Seki K (2010) Radiofrequency ablation as local therapy for early breast carcinomas. Breast Cancer. doi:10.1007/s12282-009-0186-9
4. Fornage BD, Sneige N, Ross MI, Mirza AN, Kuere HM, Edeiken BS, et al. Small (≤2-cm) breast cancer treated with US-guided radiofrequency ablation: feasibility study. Radiology. 2004; 231:215–24.

Breast Cancer (2011) 18:24–32
DOI 10.1007/s12282-010-0222-9



# A histopathological study for evaluation of therapeutic effects of radiofrequency ablation in patients with breast cancer

**Hitoshi Tsuda · Kunihiko Seki · Takahiro Hasebe · Yuko Sasajima · Tatsuhiro Shibata · Eriko Iwamoto · Takayuki Kinoshita**

Received: 20 July 2010 / Accepted: 24 August 2010 / Published online: 23 September 2010


**Abstract**
*Purpose* To reveal the rate of complete therapeutic effect of radiofrequency ablation (RFA) and its correlation with tumor size by the histopathological examination of surgically resected early breast cancers.
*Methods* For 28 patients who received RFA and subsequent surgical therapies for early breast cancer treatment, the effect of RFA was evaluated by both histopathological examination and nicotinamide adenine dinucleotide (NADH)-diaphorase staining of resected tumor specimens according to the criteria described by Seki et al. (this issue). The correlation of 100% RFA effect with tumor parameters including tumor size and the presence of extensive intraductal component (EIC) was examined.
*Results* The mean size and invasive size of the primary tumors were 2.21 cm (ranging from 0.6 to 5.0 cm) and 1.44 cm (ranging from 0 to 5.0 cm), respectively. By examining hematoxylin-eosin (HE) sections, the effectiveness of RFA was found to be 100% in 16 tumors (57%). However, the effectiveness of RFA was found to be 100% in 22 cases (79%) examined by NADH-diaphorase staining of frozen sections containing part of tumorous and nontumorous tissues. The accuracy of diagnosis of complete RFA effect using NADH-diaphorase staining with reference to HE was 79% (22 of 28) with 100% (16 of 16) sensitivity and 50% (6 of 12) specificity. The rate of 100% RFA effect by HE examination was higher in EIC(−) tumors (13 of 17, 76%) than in EIC(+) tumors (1 of 9, 11%) ($P = 0.0022$), and was higher in tumors of $\leq$1.5 cm (10 of 11, 91%) than in tumors of >1.5 cm (6 of 17, 35%; $P = 0.0034$). All five tumors of $\leq$1.0 cm showed 100% RFA effect, but 3 (27%) of 11 tumors of >1.0 and $\leq$2.0 cm and 9 (75%) of 12 tumors of >2.0 cm showed suboptimal RFA effect by HE.
*Conclusions* Tumor size of $\leq$1.5 cm, strictly $\leq$1.0 cm, could be an indication for RFA if a complete histological therapeutic effect is mandatory.

**Keywords** Radiofrequency ablation · Breast cancer · Therapeutic effect · NADH diaphorase

H. Tsuda (✉) · T. Hasebe · Y. Sasajima · T. Shibata
Pathology and Clinical Laboratory Division, National Cancer Center Hospital, 5-1-1 Tsukiji, Chuo-ku, Tokyo 104-0045, Japan
e-mail: hstsuda@ncc.go.jp

K. Seki
Clinical Laboratory Division, JR Tokyo General Hospital, 2-1-3 Yoyogi, Shibuya-ku, Tokyo 151-8528, Japan

T. Hasebe
Pathology Consultation Service, Clinical Trials and Practice Support Division, Center for Cancer Control and Information Services, National Cancer Center, 5-1-1 Tsukiji, Chuo-ku, Tokyo 104-0045, Japan

T. Shibata
Cancer Genomics Project, Center for Medical Genomics, National Cancer Center Research Institute, 5-1-1 Tsukiji, Chuo-ku, Tokyo 104-0045, Japan

E. Iwamoto · T. Kinoshita
Surgical Oncology Division, National Cancer Center Hospital, 5-1-1 Tsukiji, Chuo-ku, Tokyo 104-0045, Japan

## Introduction

Histopathological evaluation of radiotherapeutic effects in patients' cancerous tissues, including esophageal or cervical cancers, was established in Japan in the 1960s [1]. This system evaluates the percentage of area with markedly altered, presumably nonviable cancer cells, and the area

**Table 1** Pathological findings and therapeutic effects in 28 tumors subjected to radiofrequency ablation (RFA)

| No./age | Permanent section | | | | | | | | | | | | Frozen section | |
|---|---|---|---|---|---|---|---|---|---|---|---|---|---|---|
| | Histology | Grade | pN | ER | PR | HER2 | Tumor size (cm) | Invasive size (cm) | Daughter nodule | EIC | Area with RFA effect (cm) | RFA effect (HE) (%) | Tumor size in sample | NADH effect (%) |
| 1/52/L | muc | 1 | 0 | 2 | 0 | 1 | 2.4 | 2.4 | – | – | 6.6 | 100 | 1.6 | 100 |
| 2/69/R | Pred DCIS | 1 | 0 | 3 | 1 | 1 | 2.2 | 0.08 | – | NA | 3.2 | 100 | 0.8 | 100 |
| 3/79/R | IDC(pap) | 2 | 0 | 3 | 3 | 0 | 2.1 | 2.1 | – | – | 6 | 100 | 1.2 | 100 |
| 4/67/L | IDC(sol) | 3 | 0 | 0 | 0 | 0 | 2 | 1.7 | – | – | 4.2 | 100 | 1.7 | 100 |
| 5/64/R | IDC(sol) | 3 | 0 | 0 | 0 | 1 | 1.7 | 1 | – | – | 5.5 | 100 | 1.3 | 100 |
| 6/68/L | IDC(sci) | 3 | 0 | 0 | 0 | 0 | 1.6 | 1.6 | – | – | 3.5 | 100 | 1.3 | 100 |
| 7/54/L | IDC(pap) | 1 | 0 | 3 | 1 | 1 | 1.5 | 0.8 | – | + | 5.8 | 100 | 0.3 | 100 |
| 8/62/L | IDC(sol) | 2 | 0 | 3 | 3 | 0 | 1.5 | 1.5 | + | – | 2.7 | 100 | 1.3 | 100 |
| 9/53/R | IDC(sci) | 2 | 0 | 3 | 3 | 0 | 1.3 | 1.3 | – | – | 2.8 | 100 | 1.1 | 100 |
| 10/36/R | IDC(pap) | 1 | 0 | 2 | 0 | 0 | 1.2 | 1.2 | – | – | 3.4 | 100 | 0.9 | 100 |
| 11/82/R | IDC(sci) | 1 | 0 | 2 | 3 | 1 | 1.1 | 1.6 | – | – | 4 | 100 | 1 | 100 |
| 12/47/L | IDC(pap) | 1 | 0 | 3 | 3 | 1 | 1 | 0.7 | – | – | 1.9 | 100 | 1 | 100 |
| 13/66/R | DCIS | NA | 0 | 0 | 0 | 1 | 0.9 | 0 | – | NA | 4 | 100 | 0.8 | 100 |
| 14/67/L | IDC(sci) | 2 | 1 | 3 | 2 | 1 | 0.8 | 0.8 | – | – | 3.7 | 100 | 0.9 | 100 |
| 15/42/R | IDC(pap) | 1 | 1 | 2 | 2 | 0 | 0.6 | 0.5 | – | – | 3 | 100 | 0.7 | 100 |
| 16/38/L | IDC(pap) | 1 | 0 | 1 | 0 | 1 | 0.5 | 0.2 | – | – | 2.4 | 100 | 0.5 | 100 |
| 17/52/R | IDC(sci) | 1 | 3 | 3 | 3 | 0 | 5 | 5 | – | – | 5 | 90–95 | 2 | 90–95 |
| 18/45/L | IDC(pap) | 1 | 3 | 1 | 3 | 1 | 4.7 | 1.1 | + | + | 3.9 | 30 | 0.5 | 100 |
| 19/57/L | IDC(sol) | 1 | 0 | 3 | 2 | 0 | 4.7 | 2.1 | – | + | 1.7 | 40 | 0.7 | 90 |
| 20/78/R | IDC(pap) | 1 | 1 | 3 | 0 | 0 | 4.2 | 1.2 | – | + | 4.7 | 95 | 1.2 | 100 |
| 21/48/R | IDC(sci) | 2 | 0 | 1 | 3 | 0 | 4 | 2.4 | – | + | 4 | 60 | 1.3 | 90 |
| 22/59/L | IDC(sol) | 3 | 0 | 0 | 0 | 3 | 3.5 | 2.6 | – | + | 3.9 | 40–50 | 1.5 | 40–50 |
| 23/62/R | IDC(pap) | 1 | 0 | 3 | 3 | 1 | 3.2 | 1.1 | – | + | 2.6 | 60–70 | 1.6 | 80 |
| 24/73/L | IDC(sci) | 1 | 0 | 3 | 1 | 1 | 2.5 | 2.5 | – | – | 3.3 | 90 | 1.4 | 100 |
| 25/60/L | IDC(sol) | 1 | 0 | 3 | 3 | 0 | 2.5 | 1 | – | + | 2.5 | 95 | 1 | 100 |
| 26/43/L | IDC(sci) | 1 | 0 | 3 | 3 | 1 | 2 | 0.8 | – | – | 2.5 | 95 | 0.4 | 100 |
| 27/63/L | IDC(pap) | 1 | 0 | 3 | 3 | 1 | 1.8 | 1.5 | – | + | 1.7 | 80 | 1.5 | 0 |
| 28/69/L | muc | 1 | 0 | 3 | 0 | 0 | 1.5 | 1.5 | – | – | 5.5 | 95 | 1.3 | 100 |

Tumor size includes both invasive and intraductal components

*DCIS* ductal carcinoma in situ, *EIC* extensive intraductal component, *ER* estrogen receptor, *HE* hematoxylin-eosin, *HER2* human epidermal growth factor receptor 2, *IDC* invasive ductal carcinoma, *L* left, *muc* mucinous carcinoma, *NA* not applicable, *NADH* nicotinamide adenine dinucleotide-diaphorase, *pap* papillotubular carcinoma, *PR* progesterone receptor, *Pred DCIS* predominantly DCIS, *R* right, *sci* scirrhous carcinoma, *sol* solid-tubular carcinoma

from where cancer cells had disappeared [1]. The application of this classification was extended to evaluation of chemotherapeutic effects in 1985 and adopted in the 11th edition of the General Rules for the Gastric Cancer Study [2]. However, it was very difficult to determine correctly whether the altered cancer cells were viable.

In the NSABP-B-18 trial of neoadjuvant chemotherapy for patients with breast cancer, a histopathological evaluation system for chemotherapeutic effects was adopted solely on the basis of the presence or absence of invasive cancer cells, regardless of the degree of cellular degeneration or viability [3]. Thereafter, in different histopathological criteria used for evaluating therapeutic effects in breast cancers by using neoadjuvant chemotherapy, the evaluation was done usually on the basis of the presence of residual tumor cells, regardless of the extent of alteration of residual cancer cells [4, 5]. Because the sensitivity of cancer cells against chemo- or radiotherapy differs among cases, and the extent of therapeutic effects was shown to be correlated with patients' prognosis, accurate histopathological assessment of therapeutic effects has come to be required by clinical oncologists to pathologists as a routine activity. Because sometimes the pathological complete response (pCR) is set as the primary end point of clinical studies of neoadjuvant therapies to breast cancers [6–8], evaluation is frequently conducted in the form of a central pathological review [7, 8].

Recently, radiofrequency ablation (RFA) has been introduced in the field of breast cancer therapy [9, 10]. Because the effect of RFA is evaluated by cautery effect, which is almost common among tumors if the conditions of operation were uniform, establishment of common criteria for assessing therapeutic effects would be very useful to pathologists. In general, evaluation is performed by a combination of hematoxylin and eosin (HE) staining and nicotinamide adenine dinucleotide (NADH)-diaphorase

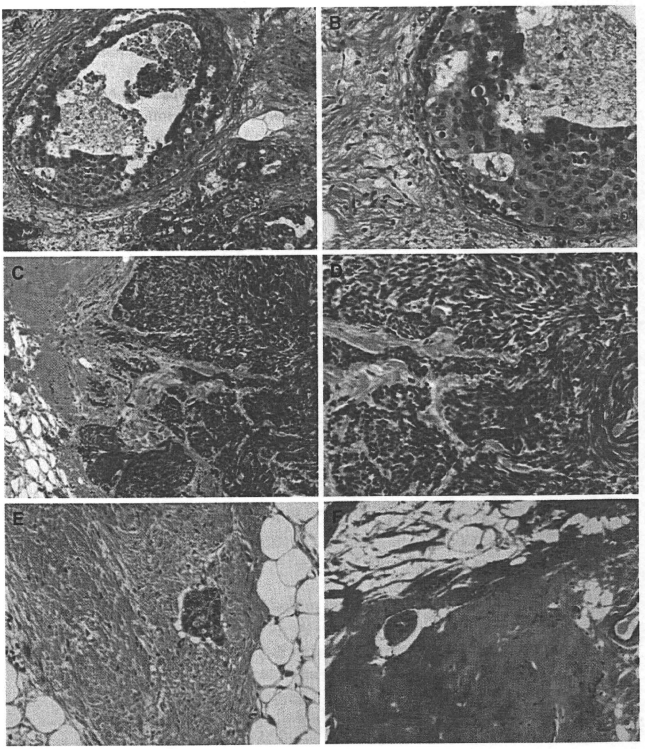


**Fig. 1** Alterations in breast cancer and noncancerous tissues by radiofrequency ablation (RFA). **a**, **b** In situ component of a ductal carcinoma without RFA effect. Cancer cells and stromal lymphocytes are viable without degenerative changes, and the morphology of stromal collagen fiber is well preserved. **c**, **d** Invasive carcinoma component with RFA effect. Cancer cells and stromal cells show pyknotic "streaming" nuclei, unclear intercellular boundaries, and unclear nuclear and cytoplasmic morphological details. In stroma, collagen fibers show degenerative changes. **e** Breast stromal tissue without RFA effect. The morphology of stromal collagen fibers is well preserved. A cancer cell nest is also seen. **f** Noncancerous stromal tissue with RFA effect. In stroma, collagen fibers show degenerative changes resulting in dense homogeneous and highly eosinophilic features. ×100 in **a**, **c**, **e**, and **f**, and ×200 in **b** and **d**. ×100 in **a** and **c**, and ×200 in **b** and **d**

staining (reviewed in ref. [11]). Although several studies have shown that evaluation of the therapeutic effects by using NADH-diaphorase staining is useful, evaluation of therapeutic effects by RFA would become more reproducible and accurate if evaluations are effectively done using HE-stained sections of formalin-fixed, paraffin-embedded tissues. Seki et al. [11] have described criteria for histopathological evaluation of RFA effects in breast cancers.

In the present study, RFA effects assessed by HE staining were compared with those assessed by NADH-diaphorase staining of surgically resected breast-cancer tissues, which were obtained immediately after RFA application in a pilot study to examine the safety and efficacy of RFA [9, 11]. In addition, we examined the parameters that caused suboptimal histopathological therapeutic effects in the tumor treated by RFA.

## Patients and methods

### RFA study protocol

This study was approved by the Institutional Review Board for ethical issues in the National Cancer Center, Japan. All the patients provided written informed consent. The criteria for patient selection and the RFA protocol have been previously described [9]. Under ultrasound guidance, RFA was performed using the 17-gauge Valleylab RF Ablation System with Cool-tip Technology (Covidien, Energy-Based Devices, Interventional Oncology, Boulder, CO) [9]. Histochemical and histopathological examinations of specimens from 28 patients who underwent RFA for primary breast cancer and subsequent partial breast resection or mastectomy between June 2008 and May 2009 were performed. For RFA, radiofrequency energy was sufficient in 19, but the increase of the energy during the procedure was suboptimal in 2 cases (cases 23 and 27 in Table 1).

After ablation, the surgically resected specimens were subjected to sampling of tumor and control tissues for NADH-diaphorase staining. From the representative cut surface of the ablated tumor, at least two thinly sliced sections 2–3 cm in size were removed and prepared as frozen sections: one section contained an apparently ablated area and a representative cut surface of the main tumor, and the other contained non-tumor areas without RFA effect. These tissues were mounted in Cryo Mount I (Muto Pure Chemicals, Tokyo, Japan), immediately frozen on dry ice, and cut into 8- to 10-μm-thick sections. One of these sections was stained with HE, and the others were stored at −80°C until NADH-diaphorase staining.

Enzyme histopathological analysis of the ablated breast tumors was performed according to a method described by Seki et al. [11] and Imoto et al. [12]. The ablated areas were confirmed to contain dead cells, which were negative for the oxidation-reduction reaction mediated by NADH-diaphorase, whereas residual live cells stained blue. We compared the histopathological features of the stained with the unstained adjacent areas by using serial sections stained with both the NADH-diaphorase reaction and HE. The histopathological features attributable to the thermal effects of RFA were investigated by two pathologists.

The remaining surgically resected specimens were fixed in 10% formalin and processed for routine histopathological examination. For partially resected breast specimens, a total of ~20–30 tissue blocks were all sectioned. For total mastectomy specimens, more than 15 tissue blocks were made, all including entire tumor areas. If necessary, additional cutting was performed after initial histological examinations. The ablated areas and ablated tumorous areas were mapped on cut sections, and on the basis of this map, the percentage areas containing tumorous tissue was estimated by at least 2 pathologists.

For both frozen sections and formalin-fixed, paraffin-embedded sections stained with HE, RFA damage to the epithelial cells and fibrous stroma was histologically evaluated according to the criteria described by Seki et al. [11]. In brief, the area with RFA effect in HE-stained sections was histologically visualized as follows (Fig. 1).

**Table 2** Summary of the profiles of 28 primary breast carcinomas subjected to radiofrequency ablation (RFA) and subsequent partial resection of the breast or mastectomy

| | |
|---|---|
| Mean tumor size (total) | 2.21 cm (0.6–5.0) (1.31 SD) |
| Mean tumor size (invasion) | 1.44 cm (0–5.0) (1.00 SD) |
| Mean size of degenerated area by RFA | 3.71 cm (1.7–6.0) (1.33 SD) |
| Incidence of 100% RFA effect by HE staining in primary tumor | 16/28 (57%) |
| Incidence of 100% RFA effect by NADH-diaphorase staining in primary tumors | 22/28 (79%) |
| Concordance between RFA effect by HE and RFA effect NADH-diaphorase staining | 22/28 (79%) |

Tumor size (total) includes both invasive and intraductal components

*HE* hematoxylin and eosin, *NADH* nicotinamide adenine dinucleotide, *SD* standard deviation

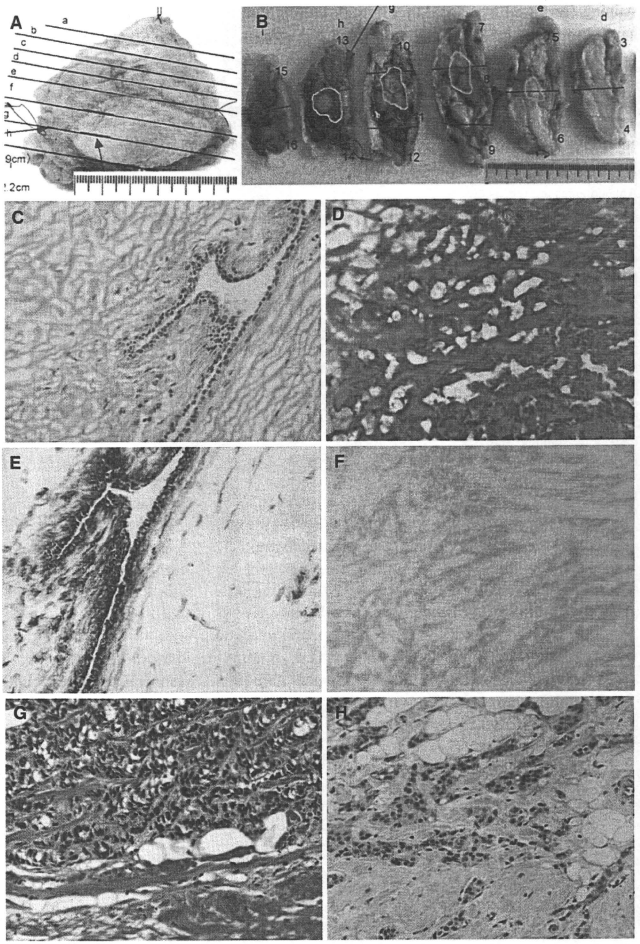


**Fig. 2** A case with 100% effective RFA in the main tumor but no effect in the daughter lesion assessed by hematoxylin and eosin (HE) staining. **a**, **b** Surgically resected specimens. *Areas* in *red* represent invasive carcinoma components. Ablated areas are circumscribed in *green*. An *arrow* indicates the daughter lesion. **c**, **d** Frozen sections of the resected tissue specimens stained with HE. **c** Viable non-tumor area with no histopathological RFA effect. No degradation changes are seen in epithelial cells and stromal structures. **d** Tumor area with a strong histopathological RFA effect. Tumor tissues had lost intercellular boundaries and nuclear or cytoplasmic morphological details. Fibrous connective tissue is also highly degenerated into a densely homogeneous and highly eosinophilic structure. **e**, **f** Nicotinamide adenine dinucleotide (NADH)-diaphorase reaction of serial sections of **c** and **d**. **e** NADH diaphorase in a histopathologically viable area. **f** NADH diaphorase in an area with highly degenerated histopathological features. **g**, **h** Permanent sections stained with HE. **g** Histopathologically highly degenerated tumor area (*upper*) and stromal area (*lower*). **h** Histopathological features of the daughter lesions in which no RFA effect is seen. ×100

Epithelial cells, both cancerous and noncancerous, were characterized by elongated eosinophilic cytoplasm with pyknotic "streaming" nuclei. The intercellular boundaries and details of the nuclear and cytoplasmic morphology were unclear (Fig. 1a–d). Fibrous connective tissue also showed degenerative changes with dense homogeneous and highly eosinophilic features. The original delicate, wavy appearance entirely disappeared. Fibroblasts in the area also showed thermal degenerative changes identical to those seen in epithelial cells (Fig. 1e, f).

Statistical analysis

Statistical difference was analyzed by Fisher's exact test.

## Results

The findings of pathological examination of the 28 tumors subjected to RFA are presented in Tables 1 and 2. In the Tables, tumor size or tumor size (total) means to the largest

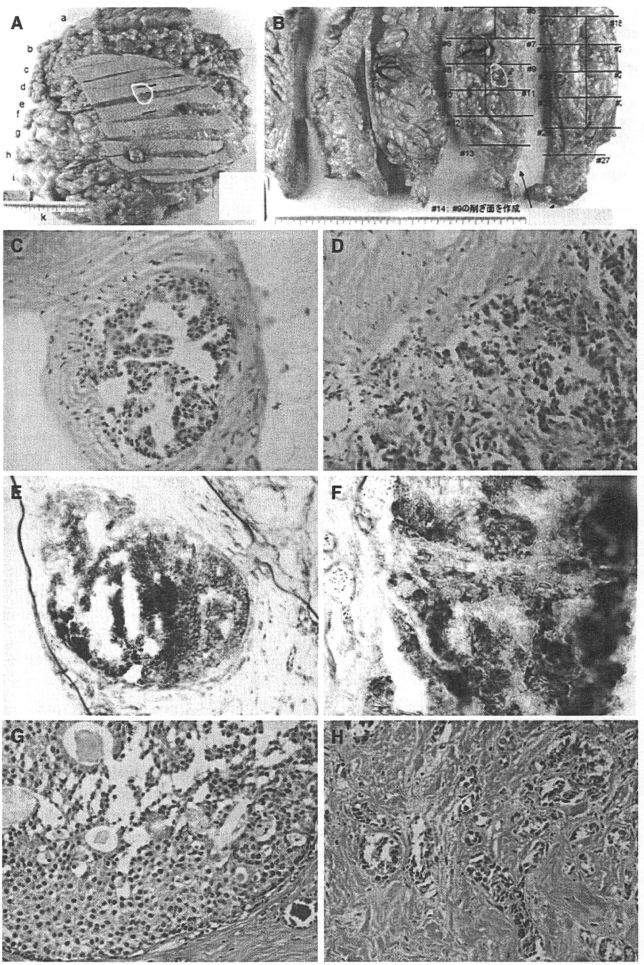


**Fig. 3** A case in which histological evaluation of RFA effect was 80% by HE, but the effect was absent by NADH-diaphorase staining. **a**, **b** Surgically resected specimens. *Areas* in *red* and *blue* represent invasive carcinoma and ductal carcinoma in situ (DCIS), respectively. Ablated areas are represented in *yellow*. **c**, **d** Frozen sections of the tumor tissue stained with HE. **c** A viable area without histopathological RFA effect. No degradation changes are seen in either tumor or stromal tissues. **d** An area with histopathological RFA effect. The cells of the tumor tissue show elongated eosinophilic cytoplasm with pyknotic nuclei. **e**, **f** NADH-diaphorase reaction. The results of NADH-diaphorase staining were positive in both histologically viable and nonviable tissue areas in series with **c** and **d**. **g**, **h** Formalin-fixed, paraffin-embedded sections stained with HE. **g** Histopathologically viable DCIS area. **h** Histopathologically highly degenerated invasive carcinoma area. Findings are the same as those in **d**; ×100 in **c** and **e**; ×200 in **d**, **f**, **g** and **h**

diameter of the tumor, including invasive carcinoma and intraductal carcinoma components and including both ablated and non-ablated tumor area. Histological grades of the tumors were 1, 2, and 3 in 18, 5, and 4, respectively. Grading of one tumor could not be determined because of marked degenerative changes. The mean tumor size, including both invasive and noninvasive components, was 2.21 cm, ranging from 0.6 to 5.0 cm. The mean size of invasive components was 1.44 cm, ranging from 0 [ductal carcinoma in situ (DCIS)] to 5.0 cm. An extensive intraductal component (EIC) was positive in 9 tumors, but negative in 17 tumors. One case of DCIS and one case of invasive ductal carcinoma with a predominantly DCIS component were included in the study.

The mean size of the degenerated areas by RFA, including both tumorous and the surrounding nontumorous

**Table 3** Factors correlated with 100% radiofrequency ablation (RFA) effect by hematoxylin eosin (HE) findings

| Factor | Number of tumors (%) RFA effect by HE | | | P |
|---|---|---|---|---|
| | Total | 100% Effect | <100% Effect | |
| Extensive intraductal component (EIC) | | | | |
| EIC(+) | 9 | 1 (11) | 8 (89) | 0.0022 |
| EIC(−) | 17 | 13 (76) | 4 (24) | |
| DCIS | 2 | 2 (100) | 0 (0) | |
| Tumor size (total, cutoff 1.5 cm)[a] | | | | |
| ≤1.5 cm | 11 | 10 (91) | 1 (9) | 0.0034 |
| >1.5 cm | 17 | 6 (35) | 11 (65) | |
| Tumor size (total, cutoff 1.0 cm and 2.0 cm) | | | | |
| ≤1.0 cm | 5 | 5 (100) | 0 (0) | 0.0037 |
| >1.0 cm, ≤2.0 cm | 11 | 8 (73) | 3 (27) | |
| >2.0 cm | 12 | 3 (25) | 9 (75) | |

Tumor size (total) includes both invasive and intraductal components

*DCIS* ductal carcinoma in situ, *EIC* extensive intraductal component

[a] One tumor of ≤1.5 cm but <100% RFA effect was 1.5 cm in diameter, and the effect was 95% by HE and 100% by NADH-diaphorase staining

tissues, was 3.71 cm, ranging from 1.7 to 6.0 cm. Incidence of a 100% effective RFA by HE was 57% (16 of 28) in primary tumors. Of these 16 cases, 1 had a daughter nodule, and because RFA was performed only for the main tumor, the therapeutic effect was 100% for the main tumor, but the effect was absent for the daughter nodule (Fig. 2). By HE, in tumors with incomplete RFA effect, the area of RFA effect was evaluated to be ≥90% in 6, whereas the area was evaluated to be <90% in 6, including 2 tumors (cases 23 and 27 in Table 1), which were potentially subjected to a suboptimal increase in energy during the RFA procedure.

Nicotinamide adenine dinucleotide-diaphorase staining was positive for all sections containing nonablated areas. In the ablated tissues, tumorous tissue, and surrounding non-tumorous tissue, the size of tumor detected by the NADH-diaphorase staining varied from 0.3 to 2.0 cm (mean 1.10 cm). The incidence of 100% effective RFA detected by NADH-diaphorase staining was 79% (22 of 28) in the primary tumors. The therapeutic effect evaluated by NADH-diaphorase staining was 100% in 22 tumors, <100% but ≥90% in 3 tumors. For the other 3 tumors, the RFA effect evaluated by NADH-diaphorase staining was ≤80%: 2 of these were patients 23 and 27, in whom the radiofrequency energy did not increase optimally. In case 27, histological evaluation of the RFA effect was 80% by HE, but the effect was absent by NADH-diaphorase staining because the results of the latter staining were positive in the entire specimen examined (Fig. 3). Concordance between HE findings and NADH findings of the RFA effect was 79% (22 of 28). The specificity and sensitivity of NADH-diaphorase results (complete or incomplete RFA effect) to HE results (complete or incomplete RFA effect) were 100% (16 of 16) and 50% (6 of 12), respectively.

A 100% effective RFA evaluated by HE staining was correlated with EIC(−) and tumor size (Table 3). A 100% effective RFA was observed in 13 (76%) of the 17 EIC(−) tumors, whereas a 100% effective RFA was observed in only 1 (11%) of the 9 EIC(+) tumors ($P = 0.0022$; Fig. 4). Two cases of DCIS showed 100% RFA effect.

Likewise, a 100% effective RFA evaluated by HE staining was correlated with tumor size, including intraductal component (Table 3): a 100% effective RFA was observed in 10 (91%) of 11 tumors of ≤1.5 cm in diameter, whereas a 100% effective RFA was observed in only 6 (35%) of 17 tumors of >1.5 cm in diameter ($P = 0.0034$). One case of ≤1.5 cm, but <100% effective RFA was 1.5 cm in diameter, and the effect was observed in 95% of the area by HE and 100% of the area by NADH-diaphorase staining.

When tumor size, including intraductal component, was stratified into three categories, 100% effects of RFA were detected in all 5 (100%), 3 (27%) of 11, and 9 (75%) of 12 in tumor groups of tumor size ≤1.0 cm, >1.0 cm but ≤2.0 cm, and >2.0 cm, respectively (Table 3). The rate of a 100% effect of RFA was significantly higher in the patients with a tumor of ≤1.0 cm in size than in those with a tumor of >1.0 cm ($P = 0.0037$).

## Discussion

In this study, we evaluated the RFA effect by both HE and NADH-diaphorase staining in 28 primary breast cancers resected from patients immediately after RFA procedures. As studied by Seki et al. [11], therapeutic effects of RFA evaluated by HE were mostly concordant with the loss of cellular viability evaluated by NADH-diaphorase staining. Because the area examined in HE-stained sections was wider (2.21 cm on an average) than the area examined in NADH-diaphorase-stained sections (1.10 cm on an average), the percentage of 100% effective RFA became lower in the former (57%) than in the latter (79%). In 1 case (case 27), there was a discrepancy in the RFA effect between the HE and NADH staining in frozen sections, but examinations of the tumor tissue in formalin-fixed sections stained with HE revealed that HE findings were concordant between frozen sections and the formalin-fixed ones. From these results, only frozen-sectioning examination did not completely and accurately clarify the status of the RFA effect in the entire tumor tissue.

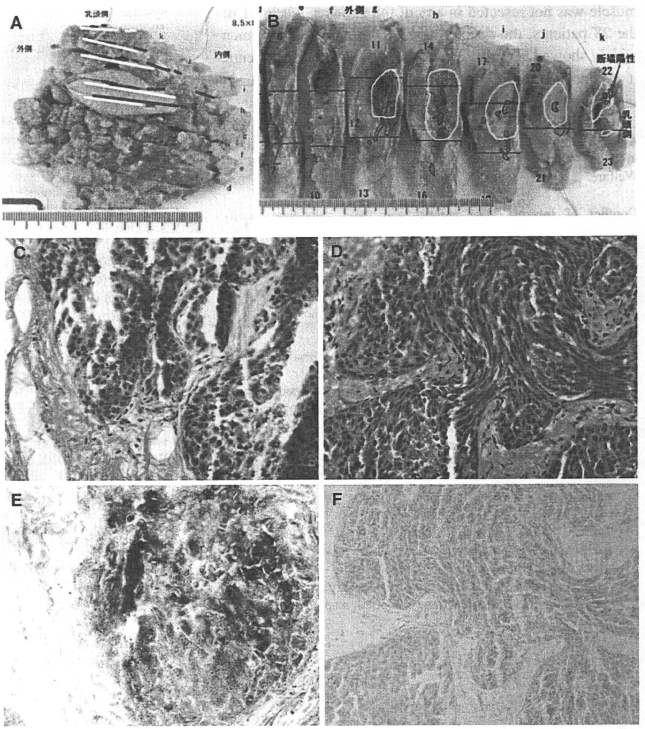


**Fig. 4** A case of breast carcinoma, extensive intraductal component (EIC)(+), with 60% effective RFA detected by HE staining of the sections. **a**, **b** Surgically resected specimens. *Areas* in *red* and *blue* represent invasive carcinoma and DCIS, respectively. Ablated areas are represented in *yellow*. **c**, **d** Frozen sections of the tumor tissue stained with HE. **c** Viable area without histopathological RFA effect. No degradative changes are seen in both tumor and stromal tissues. **d** An area with histopathological RFA effect. The cells of the tumor tissue show elongated eosinophilic cytoplasms with pyknotic "streaming" nuclei, unclear intercellular boundaries, and unclear morphological details in the nuclear or cytoplasmic features. Fibrous connective tissue also shows degenerative changes, resulting in dense homogeneous and highly eosinophilic features. **e**, **f** NADH-diaphorase reaction. **e** The results of NADH-diaphorase staining in histopathologically viable areas are positive. **f** NADH diaphorase in the area with histopathological RFA effect shows no reaction. ×200

Nonetheless, if the tumor size was small (≤1.5 cm) and the tumor lacked the EIC component, the proportion of cases with complete RFA effect became very high. In particular, complete RFA effects were observed in all tumors with a diameter of ≤1.0 cm. In these cases, if RFA therapy was conducted with subsequent follow-ups, examination of the therapeutic effect by means of core-needle/mammotome biopsy would be potentially sufficient. In contrast, the ratio of suboptimal RFA effect was high in the tumors sized 2.0 cm or larger. Even in the tumors of >1.0 cm but ≤2.0 cm in size microscopically, 27% of cases did not show a 100% of RFA effect. From the present data, tumor size of ≤1.5 cm, strictly ≤1.0 cm, could be an indication for RFA if a complete histological therapeutic effect is mandatory.

There are still challenges in determining the therapeutic effects of RFA. Judgments of the RFA therapeutic effects between HE and NADH-diaphorase staining, even by examining serial tissue sections, do not always agree. In the Chiba Cancer Center, RFA therapy and subsequent follow-up revealed cases in which HE findings showed effectiveness, but the results of NADH-diaphorase staining were positive, or cases in which HE showed no changes but the results of NADH-diaphorase staining were negative (Yamamoto N., personal communication). Data acquisition from a larger number of cases and establishment of uniform criteria for evaluation of histopathology determining therapeutic RFA effects, including researching on how the NADH-diaphorase findings should be incorporated into such criteria, are important next stages of research.

From Table 1, the diameter of the area with a RFA effect usually exceeds the tumor size by several times, including the intraductal component. The effect of RFA appeared to extend in a radial direction. We need to be concerned about the effects of this technique on the superficial and deep sides of the mammary gland. Histologically, 1 of 28 patients suffered ulceration by the heat injury on the overlying skin (no. 3 in Table 1). Pectoral

muscle was not resected in any of the patients, but in 11 of the 28 patients, the deepest area of the resected specimen widely showed a RFA effect (e.g., Fig. 4). In these patients, it is unclear if thr pectoral muscle suffered significant injury from RFA, and close follow-up is necessary.

**Acknowledgments** This work was supported in part by a grant-in-aid for scientific research from the Ministry of Health, Labor, and Welfare.

**Conflict of interest** The authors and their immediate family members have no conflicts of interest.

## References

1. Shimosato Y. Histopathological studies on irradiated lung tumors. Gann. 1964;55:521–35.
2. Japanese Research Society for Gastric Cancer. The general rules for the gastric cancer study. The 11th edition. Tokyo: Kanehara Shuppan; 1985. pp. 126–35.
3. Fisher B, Brown A, Mamounas E, Wieand S, Robidoux A, Margolese RG, et al. Effect of preoperative chemotherapy on local-regional disease in women with operable breast cancer: findings from National Surgical Adjuvant Breast and Bowel Project B-18. J Clin Oncol. 1997;15:2483–93.
4. Kuroi K, Toi M, Tsuda H, Kurosumi M, Akiyama F. Issues in the assessment of pathologic effect of primary systemic therapy for breast cancer. Breast Cancer. 2006;13:38–48.
5. Kuroi K, Toi M, Tsuda H, Kurosumi M, Akiyama F. Unargued issues on the pathological assessment of response in primary systemic therapy for breast cancer. Biomed Pharmacother. 2005; 59(Suppl 2):S387–92.
6. Buzdar AU, Ibrahim NK, Francis D, Booser DJ, Thomas ES, Theriault RL, et al. Significantly higher pathologic complete remission rate after neoadjuvant therapy with trastuzumab, paclitaxel, and epirubicin chemotherapy: results of a randomized trial in human epidermal growth factor receptor 2-positive operable breast cancer. J Clin Oncol. 2005;23:3676–85.
7. Mukai H, Watanabe T, Mitsumori M, Tsuda H, Nakamura S, Masuda N, et al. Final analysis of a safety and efficacy trial of preoperative sequential chemo-radiation therapy for the nonsurgical treatment (NST) in early breast cancer (EBC): Japan Clinical Oncology Group trial (JCOG0306). J Clin Oncol. 2010;28:7s (abstract).
8. Toi M, Nakamura S, Kuroi K, Iwata H, Ohno S, Masuda N, et al. Phase II study of preoperative sequential FEC and docetaxel predicts of pathological response and disease free survival. Breast Cancer Res Treat. 2008;110:531–9.
9. Kinoshita T, Iwamoto E, Tsuda H, Seki K. Radiofrequency ablation as local therapy for early breast carcinomas. Breast Cancer. 2010. doi:10.1007/s12282-009-0186-9.
10. Yamamoto N, Fujimoto H, Nakamura R, Arai M, Yoshii A, Kaji S, et al. Pilot study of radiofrequency ablation therapy without surgical excision for T1 breast cancer: evaluation with MRI and vacuum-assisted core needle biopsy and safety management. Breast Cancer. 2010. doi:10.1007/s12282-010-0197-6.
11. Seki K, Tsuda H, Iwamoto E, Kinoshita T. Histopathological effect of radiofrequency ablation therapy for primary breast cancer, with special reference to changes in cancer cells and stromal structure and a comparison with enzyme histochemistry. Breast Cancer. 2010. doi:10.1007/s12282-010-0215-8.
12. Imoto S, Wada N, Sakemura N, Hasebe T, Murata Y. Feasibility study on radiofrequency ablation followed by partial mastectomy for stage I breast cancer patients. Breast. 2009;18:130–4.